J. Chem. Thermodynamics 95 (2016) 195–201

Contents lists available at ScienceDirect

J. Chem. Thermodynamics

journal homepage: www.elsevier.com/locate/jct

Energetics of neutral and deprotonated (*Z*)-cinnamic acid

Juan Z. Dávalos [a,*], Carlos F.R.A.C. Lima [c,d], Artur M.S. Silva [d], Luís M.N.B.F. Santos [c], R. Erra-Balsells [b], María L. Salum [b,*]

[a] Instituto de Quimica-Fisica "Rocasolano", CSIC, Serrano 119, 28006 Madrid, Spain
[b] CIHIDECAR, Departamento de Química Orgánica, Facultad de Ciencias Exactas y Naturales, Universidad de Buenos Aires, Ciudad Universitaria, 1428 Buenos Aires, Argentina
[c] Centro de Investigação em Química, Departamento de Química e Bioquímica, Faculdade de Ciências da Universidade do Porto, P-4169-007 Porto, Portugal
[d] Department of Chemistry & QOPNA, University of Aveiro, P-3810-193 Aveiro, Portugal

ARTICLE INFO

Article history:
Received 8 September 2015
Received in revised form 9 December 2015
Accepted 12 December 2015
Available online 21 December 2015

Keywords:
(*Z*)-cinnamic acid
Enthalpies of formation
Gas-phase acidity
EKM
B3LYP
G3
G4

ABSTRACT

We have performed a study of structural, thermochemical and thermophysical properties of the (*Z*)-cinnamic acid neutral molecule and its corresponding oxyanion (formed by deprotonation of the carboxylic group). The thermophysical study (heat capacities, temperature and enthalpy of fusion) was made by DSC. The following intrinsic (gas-phase) thermochemical magnitudes have been experimentally determined: (i) standard enthalpy of formation, at $T = 298.15$ K, of the neutral molecule, $\Delta_f H^0_m(g) = (-215.5 \pm 3.2)$ kJ · mol^{-1}, by combustion calorimetry and by the Knudsen effusion technique, (ii) deprotonation enthalpy, $\Delta_{acid}H^0(g) = (1416.4 \pm 8.8)$ kJ · mol^{-1} and acidity, $GA = (1386.7 \pm 8.8)$ kJ · mol^{-1}, by the EKM method using ESI-TQ Mass Spectrometry. From these results we have also derived the enthalpy of formation of the oxyanion, $\Delta_f H^0_m$(oxyanion, g) = (-303.5 ± 9.4) kJ · mol^{-1}. A computational study, through density functional calculations at the B3LYP/6-311++G(d,p) level of theory, was used to check the good consistency of the experimental results. The global results show that (*Z*)-cinnamic acid is significantly less stable than the corresponding (*E*)-isomer, which can be related to the greater acidity of the (*Z*)-form found in both the gas and aqueous solution phases.

1. Introduction

Cinnamic acids (aryl phenylpropenoic acids) are secondary plant metabolites involved in many biosynthetic pathways of phenolic compounds such as flavonoids, stilbenes, salicylic acid and lignin [1–3]. They play important roles in plant growth and in plant-environment interactions and also function as cell wall components, UV protectors; pigments, herbicides and aroma compounds [2–4]. Furthermore, cinnamic acid derivatives have also been reported to have antibacterial, antiviral and antifungal properties [5]. The cinnamic acids can exist in both (*E*)- and (*Z*)-forms (figure 1) [1,2].

In nature, (*E*)-cinnamic acid has an important role as intermediate of the phenylpropenoid pathway which is synthesized from L-phenylalanine by phenylalanine ammonia lyase and then converted by enzymatic reactions to other metabolites [1,2,6]. On the contrary, the role of (*Z*)-cinnamic acid is still under discussion. Its presence in root tissue suggests that it may be produced through either light-dependent and independent pathways or may be transported from a plant organ to another [7]. Some authors suggested that it can be produced by UV light-mediated photo-isomerization of (*E*)-cinnamic [8] because its concentration is increased by UV irradiation of plant organs. The biological properties of (*Z*)-cinnamic acid are significantly different from those of (*E*)-forms. The (*E*)-form is generally believed to be physiologically inactive and be antagonistic to the effects of auxin in higher plants [8,9]. However, it is known that the (*Z*)-form inhibits root growth of avena, wheat, lax and arabidopsis, and also induces epinastic curvature in tomato seedlings, in the same way as the plant hormones auxin and ethylene [8,9]. Further studies have shown that (*Z*)-cinnamic acid acts on plant cells through both ethylene- and auxin-independent signalling pathways [8,9]. The role of the genes may provide some insights into the molecular mechanisms by which (*Z*)-cinnamic acid regulates plant growth and development as well as plant adaptation to environmental stresses [10].

Recently, we have developed a highly efficient one-pot preparation of (*Z*)-cinnamic acid involving an (*E*) → (*Z*) photoisomerization reaction [11,12]. Furthermore, the spectroscopic properties of (*Z*)-cinnamic acid have been studied by means of UV-visible absorption spectroscopy and high-level quantum mechanical

* Corresponding authors. Tel.: +34 915619400 (J.Z. Dávalos).
E-mail addresses: jdavalos@iqfr.csic.es (J.Z. Dávalos), mlsalum@qo.fcen.uba.ar (M.L. Salum).

http://dx.doi.org/10.1016/j.jct.2015.12.014
0021-9614/

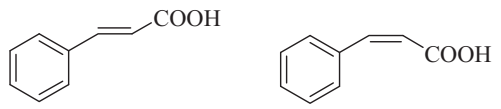

(*E*)-cinnamic acid (*Z*)-cinnamic acid

FIGURE 1. Chemical structure of (*E*)-(left) and (*Z*)-cinnamic acid (right).

computations [13]. The UV-visible absorption spectra of (*Z*)- and (*E*)-cinnamic acids reveal noticeable differences regarding the spectroscopic behaviour of both regioisomers in aqueous media. Quantum chemical calculations of the (*Z*)-form show that in aqueous solution the carboxylate group is largely out-of-plane giving a non-planar structure that modifies the electronic density delocalization, in contrast with the planar structure found for the (*E*)-form. Therefore, we decided to carry out a complete theoretical and experimental study of the thermal stability of the (*Z*)-cinnamic acid in both, its neutral and its deprotonated form (anion). The experimental thermophysical and thermochemical properties were determined using differential scanning calorimetry (DSC), static bomb (micro) combustion calorimetry and the Knudsen effusion technique. Furthermore, we determined the deprotonation parameters (acidity *GA*, deprotonation enthalpy $\Delta_{acid}H^0$ and entropy $\Delta_{acid}S^0$) by the Extended Kinetic Method (EKM), which is an improved version of the kinetic method developed by Cooks *et al.* [14] using ESI-Triple-Quadrupole Mass Spectrometry.

2. Experimental

2.1. Materials and purity control. DSC measurements

Cis-cinnamic acid or (*Z*)-cinnamic acid [(*Z*)-$C_9H_8O_2$, Z-3-phenyl-2-propenoic acid] was synthesized and purified by photoisomerization of (*E*)-cinnamic acid in acetonitrile solution, such as described elsewhere [11,12], and carefully dried under vacuum at room temperature. Chemical structure of both (*Z*)- and (*E*)-cinnamic acids were confirmed by ^{1}H NMR spectroscopy (see Supporting Information, figure S1a). Purity of the mentioned compounds was checked by their melting points [11], and also estimated by differential scanning calorimetry (DSC), which showed that the mole fraction of impurities was $<7 \times 10^{-3}$. The (*Z*)-cinnamic acid compound was studied by DSC over the T = (255.15 to 340.1) K (melting point) range, and no phase transitions were found. The heat capacities, temperature and enthalpy of fusion were experimentally determined also by DSC. Full details are given in the Supporting Information (S1). Table 1 summarizes relevant information on sample material purity.

2.2. Combustion calorimetry

The combustion experiments were performed in an *isoperibol* static *micro*-bomb calorimeter. A detailed description of this method can be found in reference [15]. The energy equivalent of the calorimeter ε(calor) was determined from the combustion of benzoic acid (NIST standard reference sample 39j), its massic energy of combustion being $(-26{,}434 \pm 3)\ J \cdot g^{-1}$, under certified conditions. From 10 calibration experiments, we obtained an ε (calor) of $(2105.3 \pm 0.3)\ J \cdot K^{-1}$, where the uncertainty quoted is the standard uncertainty of the mean.

The combustion energy of (*Z*)-cinnamic acid was determined by burning the solid samples in pellet form in oxygen at p = 3.04 MPa, with 0.05 cm^3 of water added to *micro*-bomb calorimeter. In order to obtain combustion complete reactions, Vaseline was used as auxiliary substance. The massic energy of combustion of Vaseline used was $(-46{,}086 \pm 5)\ J \cdot g^{-1}$ [16]. This value was confirmed in our laboratory. The empirical formula and massic energy of combustion of the cotton-thread fuse, $CH_{1.740}O_{0.871}$ and $(-17{,}410 \pm 37)\ J \cdot g^{-1}$ were determined in our laboratory. The uncertainty quoted corresponds to the standard deviation of the mean for ten experiments.

Corrections of apparent mass to mass, conversion of the energy of the actual bomb process to that of the isothermal process, nitric acid formation and correction to standard states were made according to Hubbard *et al.* [17]. For these corrections were used the values of density ρ = 1.23 (taken from XRD base Data), massic heat capacity $c_p = (1.202 \pm 0.002)\ J \cdot K^{-1} \cdot g^{-1}$ (taken from this work. See SI) and $(\partial V/\partial T)_p$ assumed to be $3.85 \times 10^{-7}\ dm^3 \cdot K^{-1} \cdot g^{-1}$ [18]. Complementary details are given in the Supporting Information (S2).

2.3. Enthalpy of sublimation measurements

The vapour pressures of (*Z*)-cinnamic acid as a function of temperature were measured by the combined Knudsen/Quartz crystal effusion apparatus described in detail by Santos *et al.* [19]. This methodology is based on the simultaneous gravimetric and quartz crystal microbalance mass loss detection and has the advantages of requiring smaller sample sizes and providing experimental results in shorter effusion times while allowing working temperatures of up to T = 650 K. However, due to the significant volatility of (*Z*)-cinnamic acid at low temperatures (even less than 360 K) the mass loss detection by the quartz crystal microbalance could not be achieved (sublimation of the deposited compound from the cooled quartz crystal was significant). Hence, in this case, the vapour pressures were determined through gravimetric analysis of the Knudsen cell before and after each effusion experiment. The equilibrium vapour pressures of (*Z*)-cinnamic acid were measured in the following ranges: T = (306 to 326) K and (0.08 to 0.92) Pa.

2.4. Determination of pK_a in water

The experimental titrations of (*Z*)- and (*E*)-cinnamic acids were carried out in water using a DL50 graphix (Mettler-Toledo Intl. Inc.) apparatus. A solution of 0.1 M NaOH was used as titrant and the resulting pK_a values were 4.0 and 4.45 for (*Z*)-and (*E*)-cinnamic acids, respectively.

TABLE 1
Provence and mass fraction purity of (*E*)- and (*Z*)-cinnamic acid.

Chemical	Provenance	CAS number	Mass fraction purity [a]	Purification method	Analysis method
(*E*)-cinnamic acid	Sigma–Aldrich	140-10.3	0.994	None	TLC, NMR, DSC, m.p
(*Z*)-cinnamic acid	Synthesis	102-94-3	0.996	Precipitation, filtration, ion exchange resin, evaporation	TLC, NMR, DSC, m.p.

[a] The mass fraction purity of (*E*)-cinnamic acid is based on information provided by the supplier Sigma–Aldrich. The (*Z*)-cinnamic acid was further purified as references [11,12]. The purity of both compounds was verified by TLC (thin layer chromatography), m.p. (melting point), and DSC (differential scanning calorimetry). Structural information was confirmed by NMR spectroscopy (figure S1a).

2.5. Mass spectrometry measurements. Extended kinetic method (EKM)

The experiments were carried out on a triple quadrupole (TQ) mass spectrometer Agilent/Varian 320 equipped with an electrospray ionization (ESI) source. The samples were diluted in a mixture of methanol and water with a 1:1 (vol:vol) ratio. Fresh solutions were directly infused into the ESI ionization source in the negative mode at flow rates of 10 μL/min. Approximately 5×10^{-5} M of (*Z*)-cinnamic acid and the desired reference acid were mixed in a 1:1 mass ratio. The temperatures of the drying gas and the solvents were optimized in order to promote the formation of a stronger signal of proton-bound heterodimeric anions between (*Z*)-cinnamic and reference acids. The heterodimeric anions were isolated in the first quadrupole of TQ, underwent collision-induced dissociation (CID) in the second quadrupole and the resulting fragments were analysed in the third quadrupole. CID experiments were performed using argon as collision gas (0.2 mTorr) at several ion kinetic energies in the collision cell. The centre of mass energy (E_{cm}) was calculated as: $E_{cm} = E_{lab}[m/(M+m)]$, where E_{lab} is the ion kinetic energy in the laboratory frame, m is the mass of the collision gas and M is the mass of the heterodimeric anion.

Extended Cooks Kinetic Method (EKM) [20–23]: The gas-phase acidity (or intrinsic acidity) of a protic acid AH, *GA*(AH) is defined as the Gibbs energy change for the deprotonation reaction, equation (1):

$$\begin{aligned} AH(g) \rightarrow A^-(g) + H^+(g) \quad & \Delta_{acid}G^0(1) \\ = GA, \quad & \Delta_{acid}H^0(1), \quad \Delta_{acid}S^0(1) \end{aligned} \tag{1}$$

The corresponding enthalpy and entropy changes for this reaction are referred to as gas-phase deprotonation enthalpy ($\Delta_{acid}H^0$) and deprotonation entropy ($\Delta_{acid}S^0$), respectively.

The $\Delta_{acid}H^0$ of (*Z*)-cinnamic acid was determined by the EKM method which takes into account entropic effects on the competitive dissociations of mass-selected proton-bound heterodimer anions $[A\cdots H\cdots A_{ref(i)}]^-$ generated in the gas phase, where AH is (*Z*)-cinnamic acid, $A_{ref(i)}H$ is a set of reference compounds of known *GA* and $\Delta_{acid}H^0_{ref}$. The heterodimers $[A\cdots H\cdots A_{ref(i)}]^-$ are fragmented by collision-induced dissociation (CID) in a collision cell of the spectrometer to yield the corresponding monomeric anions of the sample A^- and the reference anions $A^-_{ref(i)}$, via the two competitive dissociation channels with rate constants k and k_i, respectively. If secondary fragmentation is negligible, the abundance ratio of these fragment ions is equal to the ratio of the two dissociation rate constants, k and k_i (equation (2)).

$$A^- + A_{ref(i)}H \overset{k}{\leftarrow} [A\cdots H\cdots A^-_{ref(i)} \overset{k_i}{\rightarrow} A^-_{ref(i)} + AH \tag{2}$$

With the assumption that there are no-reverse activation energy-barriers, the acidity of the sample studied is related by a linear equation (3) which statistical procedure has been developed by Armentrout [21], and it can be expressed as,

$$\begin{aligned} \ln\left(\frac{k}{k_i}\right) &= \ln\frac{[A^-]}{\left[A^-_{ref(i)}\right]} \\ &= \frac{(\Delta_{acid}H^0_{ref(i)} - \Delta_{acid}H^{avg}_{ref})}{RT_{eff}} \\ &\quad - \left[\frac{\Delta_{acid}H^0 - \Delta_{acid}H^{avg}_{ref}}{RT_{eff}} - \frac{\Delta\left(\Delta S^0\right)}{R}\right] \end{aligned} \tag{3}$$

where, $\Delta_{acid}H^{avg}_{ref}$ is the average of the deprotonation enthalpy of the reference compounds, T_{eff} is an "effective temperature" related to the excitation energy of the dissociating $[A{\cdot}H{\cdot}A_{reg(i)}]^-$ heterodimers [24]. The entropic term $\Delta(\Delta S^0)$ can be expressed as the difference in the deprotonation entropies of the two acids [25], $\Delta\left(\Delta S^0\right) \approx \Delta_{acid}S^0 - \Delta_{acid}S^0_{ref(i)}$. If the reference compounds have similar deprotonation entropies, the last term can be substituted for the corresponding average entropy, as $\Delta\left(\Delta S^0\right) \approx \Delta_{acid}S^0 - \Delta_{acid}S^{avg}_{ref}$. We now have three unknown variables in equation (3) ($\Delta_{acid}H^0$, RT_{eff} and $\Delta_{acid}S^0$). These quantities can be obtained from two sets of thermokinetic plots based on this equation. The first set is the linear plot of $\ln(k/k_i)$ *vs* $(\Delta_{acid}H^0_{ref(i)} - \Delta_{acid}H^{avg}_{ref})$ using data collected from a series of experiments under different collision energies. The resulting plots give a series of straight lines characterized by a slope equal to $1/RT_{eff}$ and a Y-intercept including terms expressed between brackets in the equation (3). In the second thermokinetic plot, the values of the intercepts obtained in the first graph are plotted against $1/RT_{eff}$ values (obtained before). The new plot yields a second straight line with a slope given by $(\Delta_{acid}H^0 - \Delta_{acid}H^{avg}_{ref})$ and an intercept given by $-\Delta(\Delta S^0)/R$. Finally, the gas-phase acidity *GA* of sample studied is derived from equation, $GA = \Delta_{acid}H^0 - T(\Delta_{acid}S^0)$ where $T = 298.15$ K.

2.6. Computational methods

The Gaussian 09 package was used for the quantum chemical calculations. The geometries of the studied species as well as those of the reference systems used in the isodesmic reactions considered were optimized by using density functional theory (DFT), with the B3LYP hybrid functional [26] and the 6-311++G(d,p) basis set without symmetry restrictions. NBO, electrostatic potentials and harmonic vibrational frequencies were also calculated at the same level. The computed energies and enthalpies for the most stable species studied are described in detail in the Supporting Information.

Furthermore, to confirm the reliability of the measured enthalpy of formation of (*Z*)-cinnamic acid, we have obtained theoretical values evaluated using the high-level *ab initio* approaches G3 [27] and G4 [28] theories. In both methods theoretical enthalpies of formation are calculated through atomization reactions [29]. It is important to mention that the G3 theoretical procedure modifies and corrects many of the deficiencies of the Gn ($n = 1$, 2) theory and in turn, G4 improves G3 mainly in the geometry optimizations and zero-point energy corrections. The level of theory employed in the present work is expected to provide reasonable values of reaction energetics.

3. Results and discussion

3.1. Thermophysical properties

The temperature and enthalpy of fusion of (*Z*)-cinnamic acid were estimated, from three experiments, by the DSC technique as $T_{fus} = (340.1 \pm 0.6)$ K and $\Delta_{fus}H^0_m = (16.8 \pm 0.9)$ kJ · mol^{-1}, respectively. The uncertainties are expressed as combined expanded uncertainties (0.95 level of confidence).

Molar heat capacities in the condensed state $C^0_{p,m}$ (in J · K^{-1} · mol^{-1}) were measured in the range from $T = (255.15$ to $322.15)$ K (see Supporting Information). The least squares fitting of the experimental data yielded equation (4),

$$\begin{aligned} C^0_{p,m}(cd,T)/(J\cdot K^{-1}\cdot mol^{-1}) &= 0.00415\cdot(T/K)^2 \\ &\quad - 1.75516\cdot T/K + 332.709 \quad (R^2 = 0.997) \end{aligned} \tag{4}$$

3.2. Combustion calorimetry and Knudsen effusion technique. Standard enthalpies of formation of the (Z)-cinnamic acid molecule, in the gas phase, $\Delta_f H^0_m(g)$

The process involved in the combustion of (Z)-cinnamic acid is represented by reaction (5) and the experimental results are shown in table S2 of Supporting Information.

$$(Z)-\text{Cinnamic acid(cd)} + 10O_2(g) \rightarrow 9CO_2(g) + 4H_2O(\ell) \quad (5)$$

The standard ($p^0 = 0.1$ MPa) molar enthalpies of combustion, $\Delta_c H^0_m$(cd), and formation, $\Delta_f H^0_m$(cd), in the solid phase at temperature $T = 298.15$ K are shown in table 1. The values for the standard molar enthalpies of formation of $H_2O(\ell)$ and $CO_2(g)$ at $T = 298.15$ K are (-285.830 ± 0.042) and (-393.51 ± 0.13) kJ · mol^{-1}, respectively, and were taken from CODATA [30].

The enthalpies of sublimation were deduced from the temperature dependence of the vapour pressure (Clausius–Clapeyron equation), $\ln p = -B\cdot(T)^{-1} + A$. This equation was fitted using the least squares method to calculate the standard molar enthalpy of sublimation at the mean temperature, T_m, from $B = \Delta^g_{cd}H^0_m(T_m)/R$.

The standard molar enthalpy $\Delta^g_{cd}H^0_m$ at $T = 298.15$ K was computed using equation (6),

$$\Delta^g_{cd}H^0_m(T = 298.15\ \text{K}) = \Delta^g_{cd}H^0_m(T_m) + \int_{Tm}^{298.15} [C^0_{p,m}(g) - C^0_{p,m}(cd)]dT \quad (6)$$

where $C^0_{p,m}(g) = f(T)$ was derived from computational data at the B3LYP/6311++G(d,p) level, and $C^0_{p,m}(cd) = f(T)$ was taken from the experimental DSC results (equation (4)).

The standard molar enthalpies of sublimation and formation of Z-cinnamic acid, in the condensed and gaseous states, at $T = 298.15$ K are given in table 2.

As expected, in terms of volatility (E)-cinnamic acid $\{\Delta^g_{cd}G^0_m (T = 298.15\ \text{K}) = (43.9 \pm 1.0)$ kJ · mol$^{-1}\}$ [31] is less volatile than (Z)-cinnamic acid $\{(\Delta^g_{cd}G^0_m\ (T = 298.15\ \text{K}) = (37.3 \pm 1.7)$ kJ · mol$^{-1}\}$. Despite both compounds having similar $\Delta^g_{cd}S^0_m$ $(212 \pm 2$ and $213 \pm 4)$ J · K^{-1} · mol^{-1} for (E) and (Z)-cinnamic acids, respectively) [31], the higher volatility of (Z)-cinnamic acid is driven by its lower $\Delta^g_{cd}H^0_m$; $\Delta^g_{cd}H^0_m$ for (E)-cinnamic acid, at $T = 298.15$ K, is (107.1 ± 1.0) kJ · mol^{-1} [31]. This is probably due to the fact that the (E)- configuration allows for the establishment of strong intermolecular hydrogen bonds without compromising significantly the crystal packing and the molecular geometry.

3.3. Experimental ion energetics and acidity of (Z)-cinnamic acid

To determine the gas-phase acidity of (Z)-cinnamic acid by the EKM method, we have chosen five reference acids $A_{ref(i)}H$ with *GA*s ranging from (1380.3 to 1392.9) kJ · mol^{-1} (see Supporting Information): 4-hydroxybenzoic acid, methyl-4-hydroxybenzoate; 2,3,5,6-tetramethylbenzoic acid, *m-tert*-butylbenzoic acid and *p-tert*-butylbenzoic acid. The CID branching ratio of the product ions were recorded at eleven collision energies (E_{cm}), from (0.75 to 3.25) eV. The natural logarithms of the branching ratios, $\ln([A^-]/[A^-_{ref(i)}])$, were plotted against the values of $(\Delta_{acid}H^0_{ref(i)} - \Delta_{acid}H^{avg}_{ref})$ (first thermokinetic plot depicted in figure 2, left) where $\Delta_{acid}H^{avg}_{ref} = (1414.9 \pm 8.8)$ kJ · mol^{-1} is the average of the deprotonation enthalpies of reference acids (see Supporting Information). The data are fitted by a set of eleven regression lines, each one corresponding to experiments done with collision energies E_{cm}. The second thermokinetic plot (figure 2 right) is generated by plotting the negative Y-intercept values (related to the expression between brackets in equation (3)) *vs* slopes, $1/RT_{eff}$, obtained from the results of the first graph. The deprotonation thermochemical values of (Z)-cinnamic acid (table 3) were derived from the slope and the negative Y-intercept values of the linear fit of the second plot (see Supporting Information).

TABLE 2
Experimental values for the standard ($p^0 = 0.1$ MPa) molar enthalpies of: combustion, formation (in the condensed and gaseous states) and sublimation, at $T = 298.15$ K, of (Z)-cinnamic acid. All values are given in kJ · mol^{-1}.

$\Delta_c H^0_m$(cd)/ kJ · mol^{-1}	$\Delta_f H^0_m$(cd)/ kJ · mol^{-1}	$\Delta^g_{cd}H^0_m$/ kJ · mol^{-1}	$\Delta_f H^0_m$(g)/ kJ · mol^{-1}
-4368.4 ± 2.8 [a]	-316.5 ± 3.0 [a]	101.0 ± 1.2 [b]	-215.5 ± 3.2 [c]

[a] Uncertainties associated are combined expanded uncertainties of the mean (0.95 level of confidence) and include the contributions from the calibration with benzoic acid and from the combustion energy of the auxiliary materials used.
[b] Uncertainty associated was assumed to be equal to that for $\Delta^g_{cd}H^0_m(T_m)$ in equation (6), which was calculated from the standard deviation of the respecting the ln $p = f(1/T)$ linear regression.
[c] The uncertainty quoted is the combined standard uncertainty.

3.4. Structures and thermochemical properties of the neutral (Z)-cinnamic acid molecule

(Z)-Cinnamic acid has three relevant stable rotamers, **I**, **II** and its enantiomer **II′** (depicted in figure 3). In enthalpic terms **I** and **II** (or **II′**) differ by 9.7 kJ · mol^{-1}, the latter being less stable. The geometrical arrangement of the rotamers are described basically by the α, θ and ω dihedral angles, related to rotation around the $C_{1(Ph)}$–C_7, $C_7 = C_8$, C_8–C_9 bonds, respectively. **I** exhibits a planar structure ($\alpha = \theta = \omega = 0°$), whereas **II** ($\alpha = -36.2°$, $\theta = -6.0°$, $\omega = 169.4°$) and **II′** ($\alpha = +36.2°$, $\theta = +6.0°$, $\omega = -169.3°$) have a twisted structure with the propenoic fragment rotated with respect to the phenyl ring. The equilibrium constant of pertaining to the reaction **I** **II** (**II′**), is 0.0314. It follows that *ca.* $T = 298.15$ K, a sample of gaseous (Z)-cinnamic acid is an equilibrium mixture of approximately 94% and 6% of **I** and **II** (**II′**), respectively.

In the solid state, four polymorphic forms of (Z)-cinnamic acid having different melting temperatures: (305.15, 315.15, 331.15 and 341.15) K have been reported (cited in reference [33]). According to this information our sample would be the polymorph with the highest melting temperature. From XRD data of crystals of two polymorphs having $T = (331.15$ and $341.15)$ K melting temperatures, Lee *et al.* [34,35] showed that there are two independent molecules in the asymmetric unit crystalline cells. The two molecules are hydrogen bonded through carboxylic acid groups and none of them has a planar structure. Their geometric differences are the torsion angles and the bond lengths. There are significant deviations between theoretical and XRD-experimental values of geometrical parameters of (Z)-cinnamic acid. These deviations can be attributed to the fact that the theoretical calculations refer to the gas phase, whereas the experimental structures are determined in the solid state, where packing and intermolecular interactions can modify the structural properties of the molecule.

The consistency of the enthalpy of formation in the gas phase, $\Delta_f H^0_m(g)$, of (Z)-cinnamic acid was checked by atomization and isodesmic reactions. The values calculated using G3 and G4 theories – for the atomization method- were, respectively $(-211.8$ and $-211.4)$ kJ · mol^{-1}. These values are close to the experimental one (the differences are less than 4 kJ · mol^{-1}). On the other hand, the $\Delta_f H^0_m(g)$ deduced from homodesmotic (equation (7)), "bond separation isodesmic" (BSI) [36] (equation (8)) and other isodesmic reactions (equations (9) and (10)) were also close to the experimental value, the deviations being less than 6.5 kJ · mol^{-1} for equations (7) and (8); and only 1.6 kJ · mol^{-1} for equations (9) and (10). For reference compounds, we have taken the following

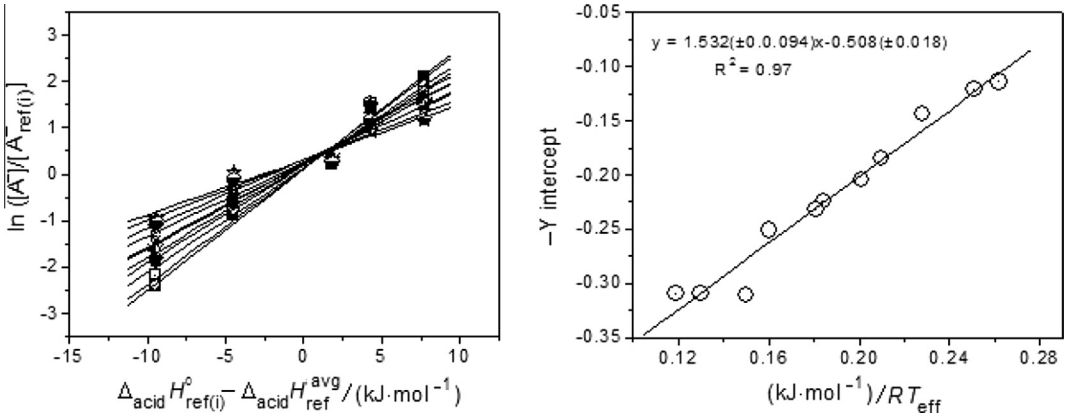

FIGURE 2. First (left) and second (right) sets of thermokinetic plots using data of CID dissociation of heterodimers $[A{\cdot}H{\cdot}A_{ref(i)}]^-$, where AH = (*Z*)-cinnamic acid and $AH_{ref(i))}$ reference compounds.

TABLE 3
Experimental and theoretical values of deprotonation thermochemical quantities for (*Z*)-cinnamic acid. The values for (*E*)-cinnamic acid are shown between brackets (data taken from reference 23).

	$\Delta_{acid}G^0(GA)$/kJ · mol^{-1}	$\Delta_{acid}H^0$/kJ · mol^{-1}	$\Delta_{acid}S^0$/J · K^{-1} · mol^{-1}	$\Delta_f H^0_m$ (oxyanion, g)/kJ · mol^{-1}
Experimental	1386.7 ± 8.8[a,b]	1416.4 ± 8.8 [a]	99.6 ± 8.4 [c]	−335.3 ± 9.4 [d]
	[1399.5 ± 8.4]	[1428.0 ± 8.4]	[96.2 ± 8.4]	[−338.0 ± 8.6] [d]
Calculated [e]	1379.8	1411.8	107.7	
	[1390.8]	[1426.8]	[110.9]	

[a] Uncertainties associated are assumed to be equal to that for $\Delta_{acid}S^{avg}_{ref}$ (See Supporting Information).
[b] Evaluated using the expression $\Delta G^0 = \Delta H^0 - T\,\Delta S^0$, with T = 298.15 K.
[c] Uncertainty associated was assumed to be equal to that for $\Delta_{acid}S^{avg}_{ref}$ (See Supporting Information).
[d] Determined using equation1 and considering $\Delta_f H^0_m$ (H^+, g) = 1536.25 ± 0.04 kJ · mol^{-1} [32].
[e] Calculated at B3LYP/6-311++G(d,p) level of theory, taking into account the contribution of populations of neutral and protonated conformers.

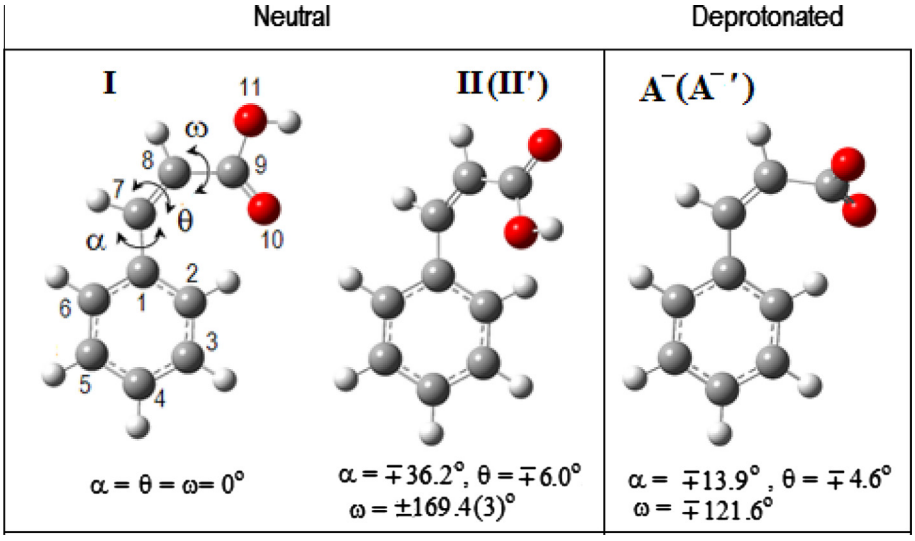

FIGURE 3. Molecular geometry of the stable conformers of neutral and deprotonated (*Z*)-cinnamic acid optimized at the B3LYP/6-311++G(d,p) level.

experimental $\Delta_f H^0_m$(g) values all in kJ · mol^{-1}: methane (−74.87 ± 0.34), ethane (−84.0 ± 0.4), ethene (52.47 ± 0.30) and formaldehyde (115.9 ± 6.3), from Chase [32]; methanol (−201.5 ± 0.2), acetic acid (−432.8 ± 2.5), styrene (148.0 ± 1.4) and toluene (50.5 ± 0.5) from Pedley [37] and (*E*)-cinnamic acid (−229.8 ± 1.9) from Dávalos *et al.* [38].

(*Z*) − cinnamic acid → (*E*) − cinnamic acid (7)

Z-cinnamic acid + 11 methane
→ 5 ethane + 4 ethene + methanol + formaldehyde (8)

Z-cinnamic acid + 2 methane → ethene + aceticacid
+ toluene (9)

Z-cinnamic acid + methane → acetic acid + styrene (10)

The enthalpy of the homodesmotic reaction 7, $\Delta_r H^0(7) = (-14.3 \pm 3.7)$ kJ · mol^{-1}, indicates that the neutral (*Z*)-form is clearly less stable than the (*E*)-form.

3.5. Intrinsic (gas phase) acidity of (Z)-cinnamic acid: structural and energetic features of the deprotonated anion (oxyanion)

The structure of the stable anion ($\mathbf{A}^-$) formed by OH-deprotonation [(*Z*)-oxyanion] is more similar to **II** than to **I** (figure 3). Rotation of the carboxylic deprotonated group moiety of $\mathbf{A}^-$ ($\alpha = -13.9°$, $\theta = -4.3°$, $\omega = -121.6°$) around the C_8-C_9 bond leads to the formation of its enantiomer $\mathbf{A}^{-\prime}$ ($\alpha = +13.9°$, $\theta = +4.3°$, $\omega = +121.6°$). Upon deprotonation of the carboxylic group, there are some significant variations in the geometrical parameters of the (*Z*)-oxyanion with respect to those of the neutral molecule: (i) almost 0.0061 nm elongation of $C_8-C_{9(COOH)}$ bond length, (ii) the $C_{1(Ph)}-C_7 = C_8$ angle decreases by more than 3°. All these changes are related to the charge redistributions which take place within the oxyanion, where there is a concentration of negative charge, particularly on the oxygen atoms O_{10} and O_{11}. Indeed, this is confirmed by the NBO charge distribution calculations, the natural charges on atoms O_{10} and O_{11} being, respectively, −0.742 and −0.770 electronic units. This charge concentration is smaller in the (*E*)-oxyanion case (−0.433 and −0.457, see Supporting Information). This could explain why the planar (*E*)-oxyanion is slightly more stable than the twisted (*Z*)-oxyanion, since the planar geometry of the *E*-form allows for more electron delocalization, which leads to a lower charge concentration on the oxygens and also a higher stability. An examination of the electrostatic potential of both (*Z*)-and (*E*)-oxyanions shows that for both anions the negative potential areas (red) are concentrated on the oxygen atoms (figure 4).

In the gas phase, we found that the (*Z*)-form is more acidic than the (*E*)-form: the experimental *GA* value of the (*Z*)-form is almost 13 kJ · mol^{-1} lower. This value is related to the stability of both neutral and anionic species (equation (1)). According to our results (table 3), the enhanced acidity of the (*Z*)-form can be attributed to the relative stabilization of its neutral molecule, which is clearly less stable than the (*E*)-form, as confirmed by the $\Delta_r H^0(7)$ value; whereas the (*Z*)- and (*E*)-oxyanions have practically the same stability, since $\Delta_f H^0_m$(*E*-oxyanion,g) is only 2.7 kJ · mol^{-1} lower than $\Delta_f H^0_m$(*Z*-oxyanion,g).

In aqueous solution, the (*Z*)-form ($pK_a = 4.0$) is also more acidic than the (*E*)-form ($pK_a = 4.45$), its acidity constant being almost 3 times higher; which is comparable to the value determined by Frederick *et al.* [39]. In comparative terms of standard Gibbs energies, the attenuation factor for aqueous solvent is approximately 5 times larger in the gas phase than in aqueous solution. It falls within the values determined by Dávalos *et al.* [40] and McMahon and Kebarle [41], who studied relationships between *GA* and the aqueous acidity of a wide variety of compounds including benzophenones, phenol and benzoic acid derivatives.

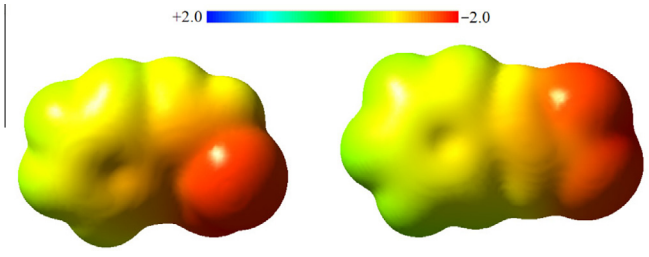

FIGURE 4. Electrostatic potential of (*Z*)- (left) and (*E*)- (right) oxyanions of cinnamic acids. Red areas correspond to negative values of the potential.

4. Conclusions

The experimental and theoretical investigation of structural effects on the thermodynamic stability of neutral (*Z*)-cinnamic acid and its anion (oxyanion, formed by deprotonation of the COOH group) are reported in this work. We have employed combustion calorimetry, the Knudsen effusion technique and DSC, to determine thermochemical and thermophysical properties of the neutral molecule, and ESI-TQ mass spectrometry (applying the EKM method) to determine the intrinsic acidity and evaluate the stability of its oxyanion. The results were supported by quantum chemical calculations at the B3LYP/6-311++G(d,p) level of theory, which confirmed the consistency of the experimental results (using *e.g.* isodesmic reactions), the good agreement between theoretical an experimental values being noticeable.

From a comparison of the thermodynamic and structural properties between the (*Z*)- and (*E*)-forms, we found that (*Z*)-cinnamic acid is:

i) less stable in the gas phase ($\Delta\Delta_f H^0_m(g) = 14.3$ kJ · mol^{-1}), (ii) more volatile, (iii) more acid, in both the gas phase ($\Delta GA = 12.8$ kJ · mol^{-1}) and in aqueous solution ($\Delta pK_a = 0.45$) phases. This difference is mainly related to the greater stability of the neutral (*E*)-form.

The similarity between the (*Z*)- and (*E*)-forms is related to: (i) the most stable neutral rotamers, which are planar molecules, (ii) the stability of their oxyanions, differing only by $\Delta\Delta_f H^0_m$(oxyanion,g) = 2.7 kJ · mol^{-1}.

Acknowledgments

The support of the Spanish MICINN Project CTQ2009-13652 is gratefully acknowledged. JZD thanks to the peruvian Grant PNICP (INNÓVATE PERÚ, ECIP-1-P-030-14). REB and MLS thank to CONICET (PIP 0072CO), UBA (X 0055BA) and ANPCyT (PICT 2012-0888) for partial financial support; both are research members of CONICET (Argentina). We thank Fundação para a Ciência e Tecnologia (FCT), Lisbon, Portugal, and European Social Fund (ESF) for financial support to CIQ, University of Porto (Projects: PEst-C/QUI/UI0081/2011 and FCUP-CIQ-UP-NORTE-07-0124-FEDER-000065), and to the Organic Chemistry Research Unit, University of Aveiro (Project: PEst-C/QUI/UI0062/2013).CFRACL thanks FCT for the award of the Research Grant SFRH/BPD/77972/2011.

Appendix A. Supplementary data

Supplementary data associated with this article can be found, in the online version, at http://dx.doi.org/10.1016/j.jct.2015.12.014.

References

[1] L. Taiz, E. Zeiger, Plant Physiology, second ed., Sinauer Associated Inc. Pub, 1998.
[2] B.B. Buchanan, W. Gruissem, R.L. Jones, Biochemistry & Molecular Biology of Plants, American Society of Plant Physiologist, Rockville, 2000 (Chapter 24, p. 1286).
[3] R.A. Dixon, Nature 411 (2001) 843–847.
[4] J.M. Humphreys, C. Chapple, Curr. Opin. Plant Biol. 5 (2002) 224–229.
[5] M. Sova, Mini Rev. Med. Chem. 12 (2012) 749–767.
[6] M.L. Salum, R. Erra-Balsells, Environ. Control Biol. 52 (2013) 1–13.
[7] Z.Q. Yin, W.S. Wong, W.C. Ye, N. Li, Chin. Sci. Bull. 48 (2003) 555–558.
[8] W.S. Wong, D. Guo, X.L. Wang, Z.Q. Yin, B. Xia, N. Li, Plant Physiol. Biochem. 43 (2005) 929–937.
[9] X.X. Yang, H.W. Choi, S.F. Yang, N. Li, Aust. J. Plant Physiol. 26 (1999) 325–335.
[10] D. Guo, W.S. Wong, W.Z. Xu, F.F. Sun, D.J. Qing, N. Li, Plant Mol. Biol. 75 (2011) 481–495.
[11] M.L. Salum, C.J. Robles, R. Erra-Balsells, Org. Lett. 12 (2010) 4808–4811.
[12] M.L. Salum, R. Erra-Balsells, Argentine Patent, CONICET #20090105020, 2009.
[13] M.L. Salum, P. Arroyo Mañez, F.J. Luque, R. Erra-Balsells, J. Photohem. Photobiol. B 148 (2015) 128–135.
[14] R.G. Cooks, T.L. Kruger, J. Am. Chem. Soc. 99 (1977) 1279–1281.

[15] J.Z. Dávalos, M.V. Roux, Meas. Sci. Technol. 11 (2000) 1421–1425.
[16] R. Sabbah, J.A.G. Perez, Thermochim. Acta 297 (1997) 17–32.
[17] W.N. Hubbard, D.W. Scott, G. Waddington, in: F.D. Rossini (Ed.), Experimental Thermochemistry, Interscience, New York, 1956 (chapter 5).
[18] W.D. Good, N.K. Smith, J. Chem. Eng. Data 14 (1969) 102–106.
[19] L.M.N.B.F. Santos, L.M.S.S. Lima, C.F.R.A.C. Lima, F.D. Magalhães, M.C. Torres, B. Schröder, M.A.V. Ribeiro da Silva, J. Chem. Thermodyn. 43 (2011) 834–843.
[20] X. Cheng, Z. Wu, C. Fenselau, J. Am. Chem. Soc. 115 (1993) 4844–4848.
[21] P.B. Armentrout, J. Am. Soc. Mass Spectrom. 11 (11) (2000) 371–379.
[22] G. Bouchoux, Mass Spectrom. Rev. 26 (2007) 775–835.
[23] A. Guerrero, T. Baer, A. Chana, J. González, J.Z. Dávalos, J. Am. Chem. Soc. 135 (2013) 9681–9690.
[24] K.M. Ervin, Int. J. Mass Spectrom. 271 (2000) 195–196.
[25] J. Ren, J.P. Tan, R.T. Harper, J. Phys. Chem. A 113 (2009) 10903–10912.
[26] C. Lee, W. Yang, R.G. Parr, Phys. Rev. B 37 (1988) 785–789.
[27] L.A. Curtiss, K. Raghavachari, P.C. Redfern, V. Rassolov, J.A. Pople, J. Chem. Phys. 109 (1998) 7764–7776.
[28] L.A. Curtiss, P.C. Redfern, K. Raghavachari, J. Chem. Phys. 126 (2007) 084108.
[29] A. Nicolaides, A. Rauk, M.N. Glukhovtsev, L. Radom, J. Phys. Chem. 100 (1996) 17460–17464.
[30] CODATA, J. Chem. Thermodyn. 8 (1975) 603–605.
[31] M.J.S. Monte, D.M. Hillesheim, J. Chem. Thermodyn. 31 (1999) 1443–1456.
[32] M.W. Jr. Chase, NIST-JANAF Thermochemical Tables, fourth ed. J. Phys. Chem. Ref. Data 1998, Monograph 9.
[33] K. Hanai, A. Kuwae, T. Takai, H. Senda, K.-K. Kunimoto, Spectrochim. Acta A 57 (2001) 513–519.
[34] H.-H. Lee, H. Senda, A. Kuwae, K. Hanai, Bull. Chem. Soc. Jpn. 67 (1994) 1475–1478.
[35] H.-H. Lee, H. Senda, K. Oyama, A. Kuwae, K. Hanai, Bull. Chem. Soc. Jpn. 67 (1994) 2574–2576.
[36] W.J. Hehre, L. Radom, P.v.R. Schleyer, J.A. Pople, Ab initio Molecular Orbital Theory, John Wiley & Sons, New York, 1986.
[37] J.B. Pedley, Thermochemical Data and Structures of Organic Compounds, Thermodynamics Research Center, College Station, TX, 1994.
[38] J.Z. Dávalos, R. Herrero, A. Chana, A. Guerrero, P. Jiménez, J.M. Santiuste, J. Phys. Chem. A 116 (2012) 2261–2267.
[39] J. Frederick, J. Dippy, R.H. Lewis, J. Chem. Soc. (1936) 644–649.
[40] J.Z. Dávalos, A. Guerrero, R. Herrero, P. Jimenez, A. Chana, J.L.M. Abboud, C.F.R. A.C. Lima, L.M.N.B.F. Santos, A.F. Lago, J. Org. Chem. 75 (2010) 2564–2571.
[41] T.B. McMahon, P. Kebarle, J. Am. Chem. Soc. 99 (1997) 2222–2230.

JCT 15-620